

# ADVANCED MATERIALS

## Supporting Information

for *Adv. Mater.*, DOI: 10.1002/adma.201701144

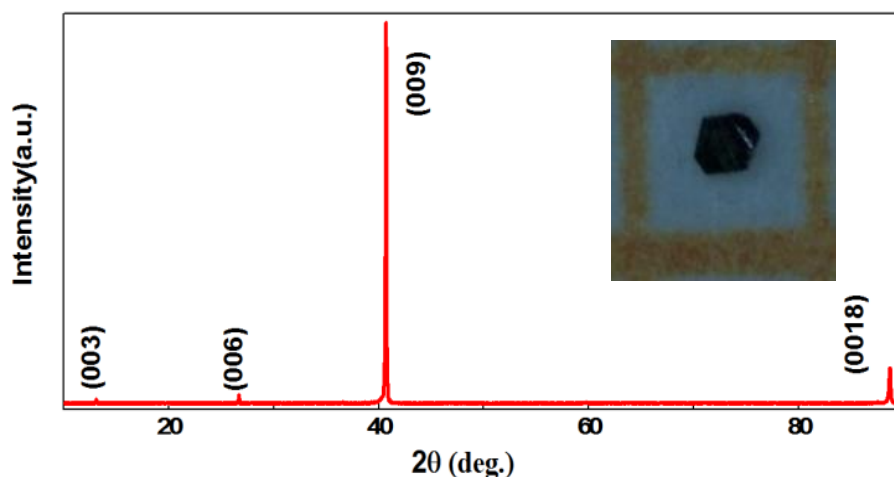
Observation of Various and Spontaneous Magnetic  
Skyrmionic Bubbles at Room Temperature in a Frustrated  
Kagome Magnet with Uniaxial Magnetic Anisotropy

*Zhipeng Hou, Weijun Ren,\* Bei Ding, Guizhou Xu, Yue Wang,  
Bing Yang, Qiang Zhang, Ying Zhang, Enke Liu, Feng Xu,  
Wenhong Wang,\* Guangheng Wu, Xixiang Zhang, Baogen  
Shen, and Zhidong Zhang*

**Supplementary Information to****Observation of Various and Spontaneous Magnetic Skyrmionic Bubbles at Room-temperature in a Frustrated Kagome Magnet with Uniaxial Magnetic Anisotropy**

*Zhipeng Hou\*, Weijin Ren\*, Bei Ding\*, Guizhou Xu, Yue Wang, Bing Yang, Qiang Zhang, Ying Zhang, Enke Liu, Feng Xu, Wenhong Wang, Guangheng Wu, Xi-xiang Zhang, Baogen Shen, Zhidong Zhang*

Single-crystal X-ray diffraction (SXRD) was performed on the crystal shown in **Figure S1** with a Bruker APEX II diffractometer using Mo K-alpha radiation ( $\lambda = 0.71073 \text{ \AA}$ ) at room temperature. Exposure time was 10 seconds with a detector distance of 60 mm. Unit cell refinement and data integration were performed with Bruker APEX3 software. A total of 180 frames were collected over a total exposure time of 2.5 hours. The crystal lattice parameters were established to be  $a = b = 5.3074 \text{ \AA}$ ,  $c = 19.7011 \text{ \AA}$  with respect to the rhombohedral unit cell (space group  $R\bar{3}m$ ), agreeing well with the previous studies. As shown in **Figure S2**, to ascertain the crystal orientations, the sample was mounted on a holder and Bruker APEX II software was used to indicate the face normal of the crystal, after the unit cell and orientation matrix were determined. One can notice that the hexagonal face is normal to  $[001]$  with the  $(100)$ ,  $(010)$ , and  $(110)$  faces around.



**FigureS1.** X-ray diffraction pattern of a  $\text{Fe}_3\text{Sn}_2$  single crystal along the perpendicular direction of hexagonal surface, which indicates that the hexagonal surface is parallel to the  $ab$ -plane and perpendicular to the  $c$ -axis. Inset: The typical photograph of  $\text{Fe}_3\text{Sn}_2$  single crystal placed on a millimeter grid. The crystal is  $0.3 \text{ mm} \times 0.3 \text{ mm} \times 0.2 \text{ mm}$  in size and possesses hexagonal mirror-like surfaces.

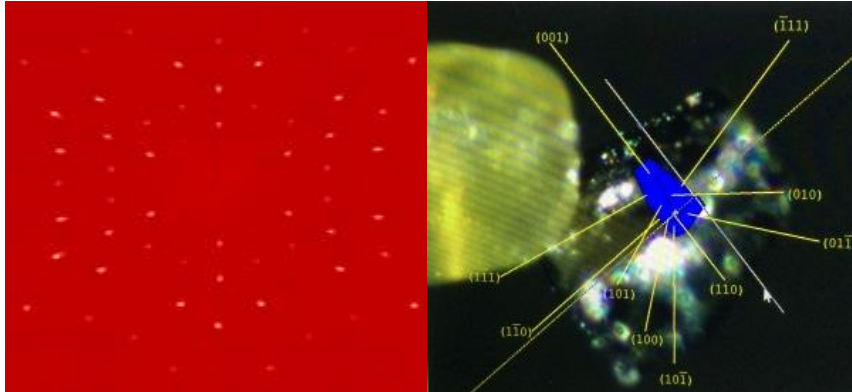


**Figure S2.** (a) Single-crystal X-ray diffraction processing image of the (00*l*) plane in the reciprocal lattice of Fe<sub>3</sub>Sn<sub>2</sub> obtained on the crystal mentioned above. No diffuse scattering is seen and all the resolved spots fit the crystal lattice structure established for Fe<sub>3</sub>Sn<sub>2</sub>. (b) Various crystal planes and their corresponding normal directions of Fe<sub>3</sub>Sn<sub>2</sub> single crystal. The yellow striped region is the glue to affix the crystal to the holder.

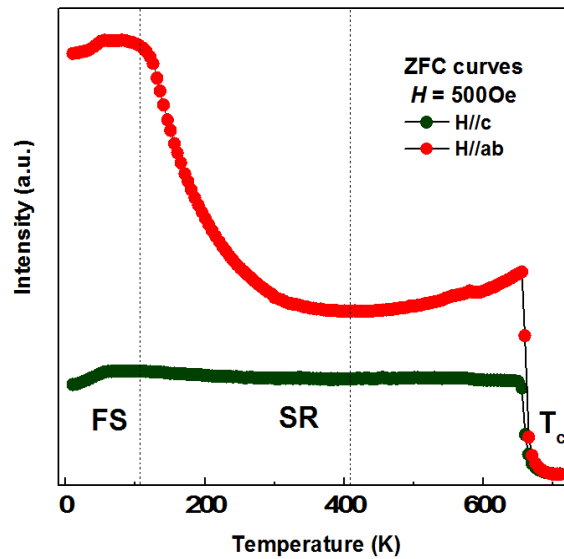


**Figure S3.** Temperature dependence of magnetization with the field-cooling (FC) model in an external magnetic field of 500Oe between 5K and 700K. As is shown in **Figure S3**, the Curie temperature  $T_c$  is established to be 660K, which is similar to previous reports. When the temperature falls below  $T_c$ , the magnetization for both magnetic fields ( $H//c$  and  $H//ab$ ) first decreases and then starts to increase at 420K, reaching a maximum at 80K. When the temperature decreases below 80K, the slight decrease in magnetization can be attributed to the entrance of the spin glass state (SGS).

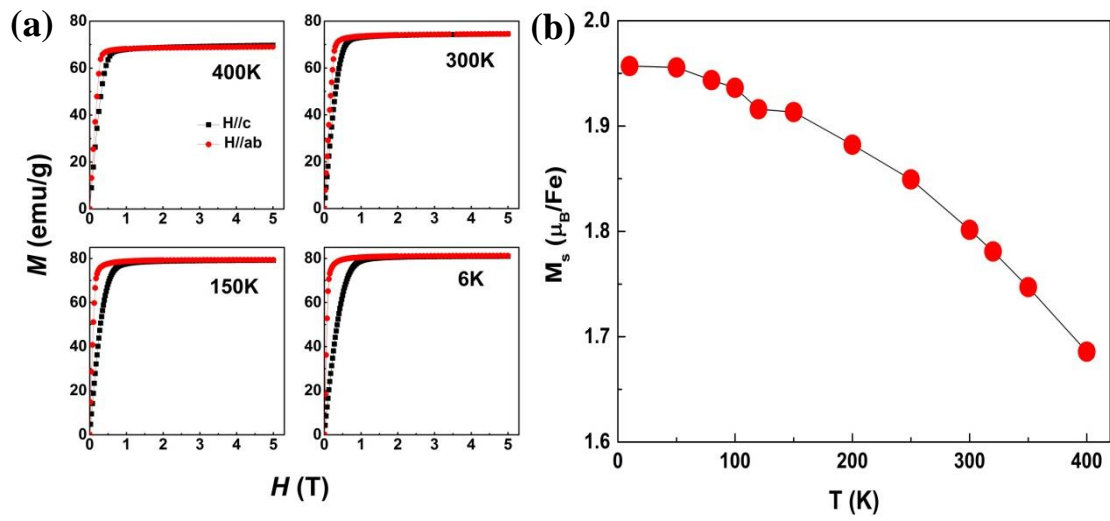


**Figure S4.** **a)** The magnetic field dependence of magnetization in fields parallel to the  $c$ -axis (black line and black symbol) and  $ab$ -plane (red line and red symbol) in the temperature range of 400K-6K. **b)** The temperature dependence of the saturation magnetization  $M_s$ .

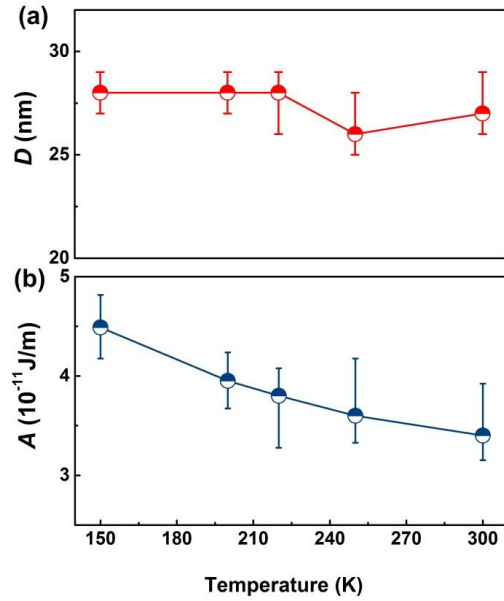
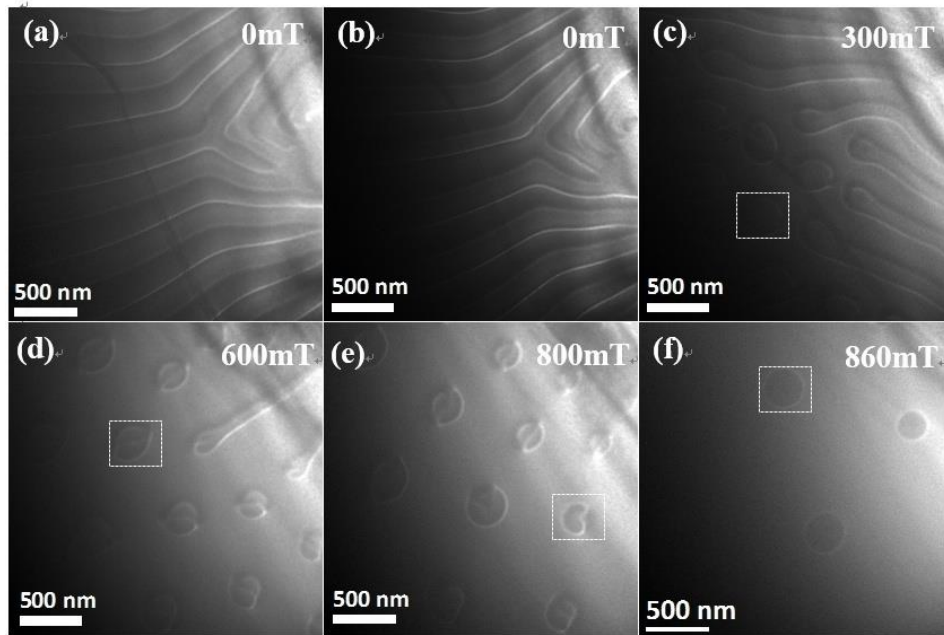


**Figure S5. a)** The temperature dependence of domain wall thickness  $D$ . The error bar denotes the deviation of three individual width measurements. One can notice that the value of  $D$  is nearly independent from the change in temperature. The exchange stiffness constant  $A$  can be established by using the equation,  $A = \frac{DK_u^2}{\pi^2}$ . **b)** The temperature dependence of  $A$ . By decreasing the temperature, the value of  $A$  increases correspondingly.



**FigureS6.** **a-b)** The over- and under-focused LTEM images under zero magnetic field at 300K. **c-f)** Corresponding under-focused TEM images for **Figure 2 (a-d)**. The boxed regions correspond to the magnetic bubbles shown in **Figure 2 (a-d)**.

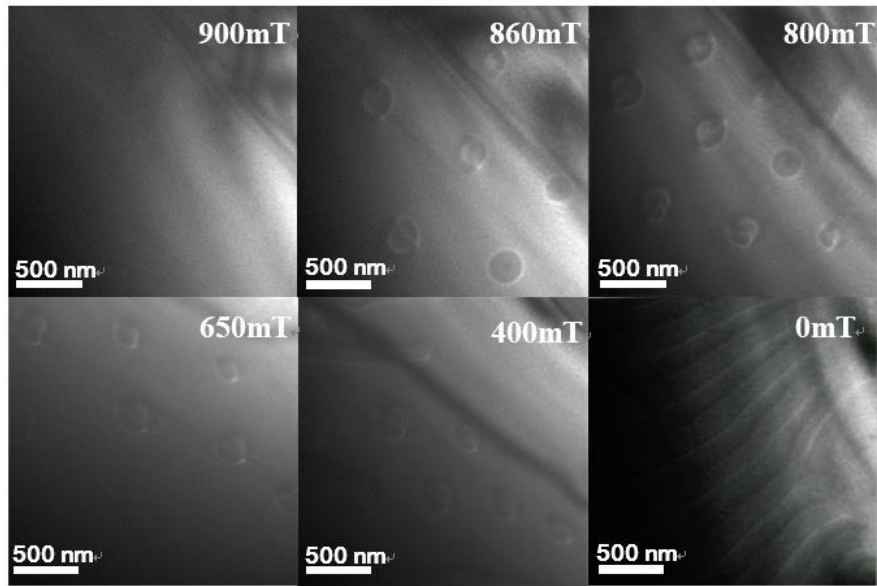


**Figure S7.** The under-focused LTEM images after a saturated magnetization. When the sample is magnetized to a saturated state, the domain reverts to the stripe.

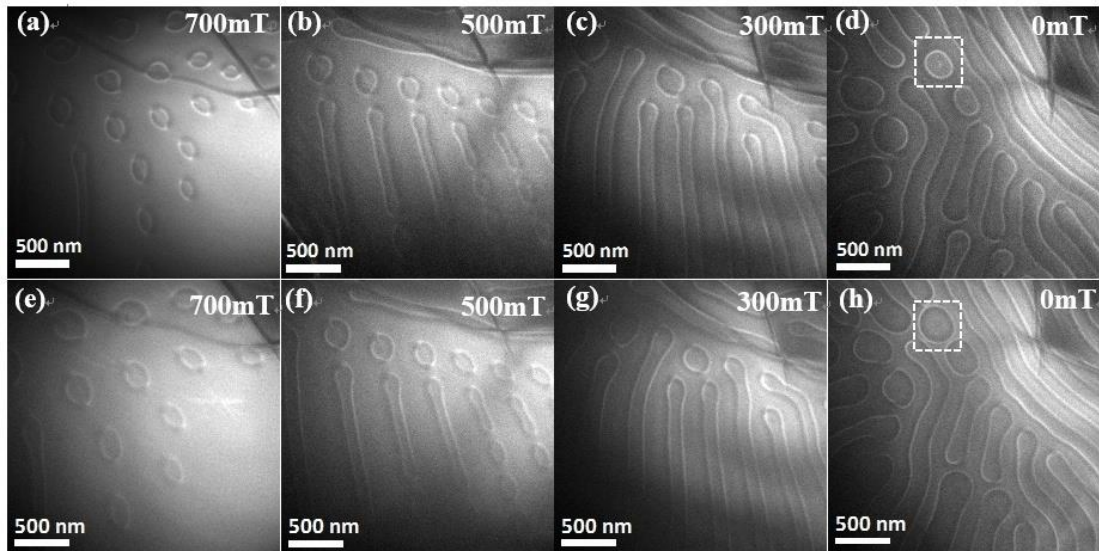


**Figure S8.** The corresponding over-focused (a, b, c, d) and under-focused (e, f, g, h) LTEM after an unsaturated magnetization in a different region from that in Figure 3. If the sample is magnetized to an intermediate state, then the skyrmionic bubbles with concentric rings appear after the magnetic field decreases to zero.